Materials Today Communications 35 (2023) 105733

Contents lists available at ScienceDirect

Materials Today Communications

journal homepage: www.elsevier.com/locate/mtcomm

Dielectric constant prediction of perovskite microwave dielectric ceramics via machine learning

Yicong Ye, Ziqi Ni *, Kaijia Hu, Yahao Li, Yongqian Peng, Xingyu Chen *

Department of Materials Science and Engineering, College of Aerospace Science and Engineering, National University of Defense Technology, Changsha 410073, China

ARTICLE INFO

Keywords:
Machine learning
Dielectric constant
Perovskite
Microwave dielectric ceramics

ABSTRACT

With the development of communication technology, microwave dielectric ceramics are in increasingly urgent need. Perovskite ceramics, as a kind of microwave dielectric ceramics with large dielectric constant span, have broad application prospects. Predicting material properties before experiments can greatly accelerate the development of materials. Although the existing methods, including classical theory and density functional theory, are of practical use for dielectric constant prediction, unsatisfactory universality and predictability limit rational design of microwave dielectric ceramics. This work aims to develop an uncomplicated method to quickly predict the dielectric constant of perovskite ceramics. According to the element and content of the compound, the dielectric constant can be accurately predicted by our machine learning model. Moreover, the model provides prediction results that are consistent with the experiment, but are completely different from those calculated by C-M equation.

1. Introduction

Microwave dielectric ceramics have been widely used in satellite television broadcasts, mobile communication, Bluetooth technology, radar, Global Position System (GPS) and other communication systems as dielectric resonators, filters, and dielectric substrates, for nearly half a century due to their excellent dielectric properties [1]. With the rapid development of mobile communication technology, especially in the past decade, the large-scale commercial use of 5 G has led to an explosive growth in the demand for microwave dielectric ceramics [2]. Dielectric constant (ε_r) is one of the most important properties of microwave dielectric ceramics, which is a physical parameter characterizing the dielectric or polarization property of dielectric materials. Different application scenarios have different requirements on dielectric properties of microwave dielectric ceramics, especially the dielectric constant. For example, ceramics with high dielectric constant can meet the demands for high-temperature capacitors [3], while ceramics with low dielectric constant are required to improve the signal transmission speed when used as dielectric substrates [4]. Therefore, in order to achieve different applications in the field of communication, it is necessary to develop potential ceramics with different dielectric constants.

Perovskite materials have attracted enormous interest because of their excellent properties, which are explained by their special structure and composition adjustability, and are widely used in solar cells [5], catalysts [6], biosensors [7], optoelectronic devices [8] and many other fields. In recent years, many excellent perovskite microwave dielectric ceramics have been reported, such as $SrTiO_3$ [9] with high dielectric constant(~200); $Ba(Zn_{1/3}Ta_{2/3})O_3$ [10] with medium dielectric constant (~30) and $(Mg_{1-x}Co_x)TiO_3$ [11] with low dielectric constant (~15). Also, perovskite microwave dielectric ceramics are in possession of properties such as low loss, adjustable temperature coefficient of resonant frequency, and have great development potential in the application of microwave components in the future. However, when the dielectric properties of perovskite ceramics are adjusted by A-site replacement [12], B-site replacement [13], or synergistic modification [14], it is difficult to achieve simultaneous adjustment of the dielectric constant, quality factor, and resonant frequency temperature coefficient. It usually takes a long time of repeated experiments to find microwave dielectric ceramics with desired properties.

Compared with the "Edison Style" that mainly relies on the experience based on the experiment, it will greatly save time and resources to predict the target performance before conducting experiments. The main methods to obtain the dielectric constant of unknown materials include experimental measurement, fitting equation and density functional theory (DFT) calculation. Experimental measurement is the most

* Corresponding authors.
E-mail addresses: niziqi18@163.com (Z. Ni), chenxingyu@nudt.edu.cn (X. Chen).

https://doi.org/10.1016/j.mtcomm.2023.105733
Received 11 November 2022; Received in revised form 3 February 2023; Accepted 28 February 2023
Available online 2 March 2023

fundamental method to obtain the actual dielectric constant of materials, but it is expensive and time-consuming. The classical Clausius Mossotti (C-M) equation bridges the gap between polarizability and dielectric constant [15], but for some materials, the calculation errors are so large that the calculated dielectric constant values are sometimes unacceptable for guiding the estimation of dielectric constant and the discovery of new dielectric materials. And other models for calculating dielectric constant, such as Penn model [16,17] and Gladstone Dale (G-D) model [18], are limited by their assumptions. DFT is one of the most commonly used calculation methods, and has been used to obtain the dielectric constant of $SnZr_{0.5}Ti_{0.5}O_3$ [19] and other materials. However, the most obvious disadvantages are that the high cost of DFT calculation and the inability to calculate complex systems.

In recent years, data-driven machine learning methods have been used in physics, materials, chemistry and other fields, and are considered as a powerful tool to predict material properties. For example, Yuan et al [20]. utilized machine learning to find ferroelectrics with excellent electrothermal effect; He et al [21]. used machine learning strategies to effectively sample ceramic powders with good piezoelectric catalytic properties; Qin et al [22]. established a high-precision prediction model for the dielectric constant of single-phase microwave dielectric ceramics through machine learning. Many literatures have reported the dielectric constant prediction based on machine learning [23,24], mostly focusing on polymers [25,26] or based on DFT calculation data [27,28]. This greatly accelerates the development process of dielectric materials. However, it is a little pity that the dielectric constant of perovskite microwave dielectric ceramics cannot be predicted directly by composition.

In this work, we predicted the dielectric constant of perovskite microwave dielectric ceramics via machine learning method. A dataset of dielectric constant of perovskite ceramics was established, features potentially related to performance were constructed and screened, and machine learning models were trained and optimized. In addition, the performance of machine learning model was compared with that of classical C-M equation in some ceramics.

2. Methods

2.1. Dataset preparing

The data used in this work were collected from the literature called *Dielectric Materials for Wireless Communication* [29] published by Dr. Sebastian in 2008. Dr. Sebastian described the state of microwave dielectric materials with a truly comprehensive list of over a thousand references at that time. We extracted 344 pieces of data of perovskite ceramics containing composition and dielectric constant, and the data of materials doped with glass or other impurities were not selected. Considering that the dielectric constant of some compounds is extremely high, the highest reaches 838, and most of the dielectric constants are relatively concentrated that the data with the dielectric constant exceeding 130 only account for 5%. To avoid problems caused by data imbalance, 19 data with the dielectric constant over 130 were eliminated, and 325 groups of data were finally retained in the dataset, with the dielectric constant ranging from 10 to 130.

2.2. Feature generation

Feature construction is the basis of machine learning process, and the quality of feature selection directly affects the results of machine learning. Therefore, it is necessary to select features that are potentially related to the dielectric constant. In the reported literature [22], chemical, structural and thermodynamic characteristics that may be related to dielectric constant were selected, but most of these characteristics need to be obtained from the Material Project database. When predicting a new material that is not included in the Material Project database, its dielectric constant cannot be estimated due to the absence of these characteristic data. Therefore, we chose the general properties of perovskite ceramics that can be calculated directly from the composition. These properties reflect the element and structure information of perovskite ceramics, which may be related to the dielectric constant. In addition, they are conveniently to obtain and contain some physical information, which has been adopted in previous studies [20,30,31]. The original 25 features extracted from the literature are shown in Table 1.

2.3. Machine learning algorithm

According to the size of our dataset, 9 commonly-used machine learning algorithms were selected, including linear regression (LR), support vector regression with linear kernel (SVR.l), support vector regression with polynomial lernel (SVR.p), support vector regression with radial basis function kernel (SVR.r), decision tree (DT), random forest (RF), AdaBoost (AdaB), Extreme Gradient Boosting (XGB) and gradient boosting decision tree (GBDT). Support vector regression is traditional strong algorithm, and RF, AdaB, XGB and GBDT are ensemble learning algorithms. For all modeling procedures, the Python programming language and Visual Studio Code software was used. The models were mainly established with scikit-learn library.

2.4. Model training and verification

The hyperparameters of the models were optimized using grid search method with the 10-fold cross validation and root mean square error (RMSE) as the scoring metric.

In order to obtain the optimal model, 127 feature combinations were generated exhaustedly to train the optimized algorithm. After the models and features were optimized, the training set and testing set were divided according to 10-fold cross validation, and the results of the testing set were predicted respectively to obtain the predictive values of all samples. When forecasting validation data, all samples were sent into the training model.

Table 1
Original selected features used in this work.

Feature	Description
ama	Relative atomic mass of A-site element[32]
amb	Relative atomic mass of B-site element[32]
ara	Atomic radius of A-site element[33]
arb	Atomic radius of B-site element[33]
bva	Ideal A-O bond distance[34]
bvb	Ideal B-O bond distance[34]
cra	Crystallographic van der Waals radii of A-site element[35]
crb	Crystallographic van der Waals radii of B-site element[35]
eaa	A-site electronegativity–absolute[36]
eab	B-site electronegativity–absolute[36]
ema	A-site electronegativity–Matyonov-Batsanov[37]
emb	B-site electronegativity–Matyonov-Batsanov[37]
epa	A-site electronegativity–Pauling[38]
epb	B-site electronegativity–Pauling[38]
era	Equilibrium van der Waals radii of A-site element[35]
erb	Equilibrium van der Waals radii of B-site element[35]
iea	Ionization energies of A-site element[39]
ieb	Ionization energies of B-site element[39]
pa	Polarizability of A-site element[40]
pb	Polarizability of B-site element[40]
ra	Ionic radii of A-site (12-coordination)[41]
rb	Ionic radii of B-site (6-coordination)[41]
t	Tolerance factor calculated by ionic radii
vea	A-site valence electron number
veb	B-site valence electron number

3. Results and discussions

3.1. Feature filter

For small size datasets, the features with high dimension will lead to high model complexity and poor generalization ability. Therefore, feature engineering should be used to filter features before training models. Here, three feature filtering methods were used, including feature filtering based on variance, feature elimination based on Pearson correlation coefficient, and feature selection based on feature importance ranking of tree models.

Variance is the average of the squares of the deviations between the values of various variables and their mean values. It is the most important method to measure the dispersion of numerical data. If the variance of a feature is very small, it means that the samples have almost no differences in this feature. Maybe most values of the feature are the same, indicating that this feature has no effect on sample differentiation. Therefore, we filtered features through variance and eliminated several features with small variance. In order to ensure the comparability between different features, each feature was normalized to an interval of 0–1 before calculating variance. The normalized variances of original features are shown in Fig. 1. The screening threshold was manually set to 0.03, and finally 18 first-generation features with variance greater than 0.03 were retained from 25 original features.

Pearson correlation coefficient can determine whether each feature is closely related. If two features are closely related, they belong to duplicate features, and only one needs to be retained. We hope that each feature in the input machine learning model is unique, so as to best represent information. Fig. 2. displayed the calculated Pearson correlation coefficient between pairs of 18 first-generation features. When Pearson correlation coefficient is greater than 0.8, it is generally believed that the two features are highly correlated. Among these features, emb, ieb, ara, and veb were not highly related to other features, so they were all retained. Then, according to the changes of RMSE after adding input features in turn, the reserved features epa and ama were selected from the two groups of highly correlation features. The remaining features had more complex interactions, which were filtered according to the model error and prior knowledge in material field. At the end of this step, 9 features were selected as the second-generation features, including emb, ieb, ara, veb, ama, epa, ra, eab, and arb. These features were arranged according to the order of screening.

Since not all features are equally important, omitting unimportant features will help further reduce the complexity of the model. We used the feature importance score based on tree model in machine learning to rank the second-generation features. Specifically, the comprehensive scores of feature importance were calculated by AdaB, GBDT, RF and XGB methods, and the results are provided in Fig. 3. The scores of the four tree models were comprehensively considered because they were obtained by different calculation methods. Importances were calculated by the Gini index and the weight in Adab, the value of the feature's importance in each single tree in GBDT, the number of splits in each tree in XGB, and the degree of decline in the accuracy of out of pocket data in RF, respectively. These highly ranked features mainly include atomic radius and electronegativity, reflecting structural and physicochemical information. Finally, the seven most important features were retained.

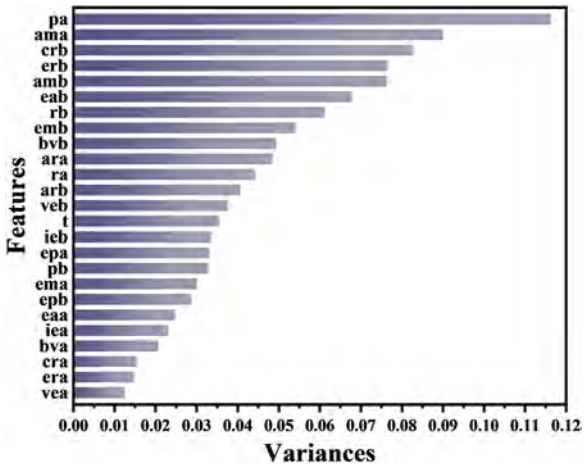

Fig. 1. Normalized variances of 25 original selected features.

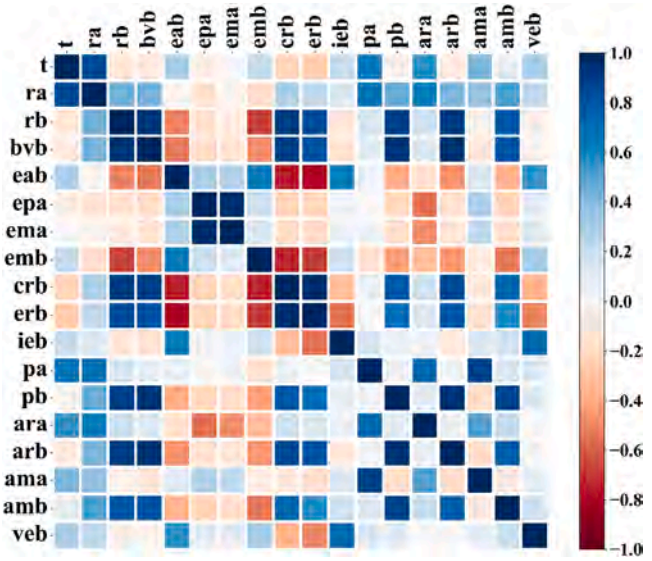

Fig. 2. Pearson correlation coefficient of 18 first-generation features.

3.2. Model performance

After the above data preprocessing and feature screening process, 325 groups of data containing one target performance and seven features were used for model training. This means that it is a small sample learning task, so it is necessary to select appropriate algorithms and tune the model.

SVR is generally recognized as a machine learning algorithm for small samples. Here we tried three kernel functions: linear kernel, polynomial kernel and radial basis function kernel. The RSME of the three models trained are 19.6, 13.5 and 10.3 respectively, as illustrated in Fig. 4. The super parameters C and gamma of SVR.r obtained by grid search are 100 and 10, respectively. Ensemble learning algorithm is to complete the learning task by constructing and combining multiple machine learners, which usually has a high accuracy in machine learning algorithms. Bagging based RF algorithm and boosting based AdaB, GBDT and XGB algorithms were used in this work. The super

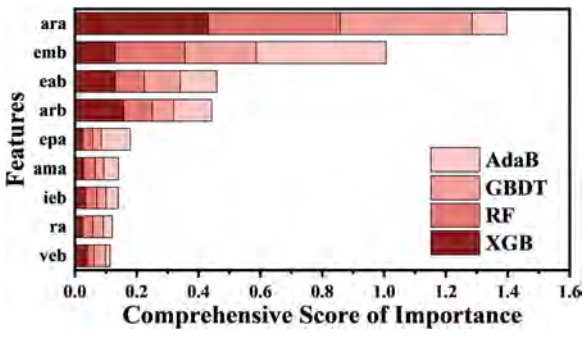

Fig. 3. Ranking list of 9 second-generation features by comprehensive score of importance calculated by AdaB, GBDT, RF and XGB methods.

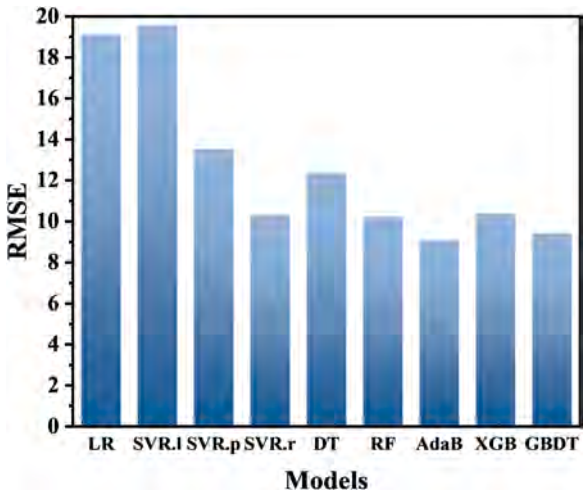

Fig. 4. RMSE of nine machine learning models compared using 10-fold cross-validation.

parameters of each ensemble algorithm, including the n_estimators and learning_rate, were optimized through grid search method. All the base estimators were DT, so the RMSE of DT was also put in Fig. 4. as a comparison. The RMSE of these 4 integrated learning models are lower than the base estimator DT and the SVR models, especially the error of Adab is as low as 9.1. The base learner of Adab is a decision tree with a maximum depth of 13, and the number of base learners is 100. It illustrates that ensemble learning is indeed a feasible method to improve the accuracy of the model. In addition, the error of linear regression (LR) model is also shown, indicating that the precisions of most machine learning models we used are higher than that of LR.

Although AdaB has the lowest RMSE, there is no significant difference between 9.1 and 10.3 for dielectric constant of microwave dielectric ceramics. Moreover, generally speaking, the generalization ability of the SVR model is better than the ensemble learning model when there are only hundreds of data. Therefore, SVR.r is considered to be the optimal machine learning algorithm. To further reduce the complexity of the model and improve the generalization ability of the model, all possible combinations of the seven most important features identified above were examined to find the subset with the lowest error for SVR.r. For each feature subset, the dataset was divided into 10 parts, and the prediction error in Fig. 5 were the average of 10 times training and prediction. Fig. 5 reflects that with the increase of the number of features, the model error initially decreases first and then increases, indicating the improvement of the model. Using more features will make the model more complex and may learn less important features. Considering "Occam shaver" principle, we used five features, including arb, eab, epa, emb and ieb, to ensure that the model had the highest accuracy and sufficient generalization ability.

We chose SVR.r algorithm and five features including arb, eab, epa, emb and ieb to train the prediction model for the dielectric constant of perovskite-type microwave dielectric ceramics. The prediction ability of the proposed model is shown in Fig. 6. Scattering points are distributed diagonally, which indicates that the model has a strong ability to capture information related to dielectric constant. The correlation between the real value and the predicted value reached 0.8837. In the field of machine learning, researchers always pursue the highest accuracy. However, in the field of materials, considering that the data in materials have different characteristics from those in other fields, we think that it may not be the most desirable result to blindly pursue the improvement of accuracy. When the accuracy of prediction reaches a certain level, how to guide the material design is a problem we want to solve more. We believe that the accuracy of the model has initially met the requirements of application. It is worth noting that for data with dielectric constant less than 60, the scatter points are concentrated near the diagonal, while for data with high dielectric constant, the scatter points are relatively more dispersed. This is the impact of the data quality of the dataset. Even though we eliminated the component points with dielectric constant greater than 130 in order to improve the data imbalance, the data in this data set is still unbalanced. Therefore, the model has better learning and higher accuracy for data with lower dielectric constant. However, in practical applications, the dielectric constant values of dielectric ceramics for most key electronic components (such as dielectric resonators in cavity filters in base stations, dielectrically loaded antenna cores, etc [42].) operating in the GHz frequency range are concentrated in the range of 20–60. Hence, this model can be used to guide the design of perovskite dielectric ceramics with lower dielectric constant. In addition, the above results reminds us that if the data quality is improved, the performance of the model can be further improved.

3.3. Model validation

In order to further verify the reliability of our model, we selected a new group of perovskite ceramics not in the data set for prediction. The dielectric constants of $(1-x)CaTiO_3$–$xLa(Mg_{2/3}Nb_{1/3})O_3$ ($x = 0.1$–0.9) ceramics sintered at their densification temperature and their dielectric constants calculated by C-M equation were given in Fig. 5 of the recently reported literature [43]. The measured values and calculated values were extracted and drawn with the values predicted by our model, as shown in Fig. 7. Interestingly, the trend of dielectric constants calculated by the classical C-M equation is completely opposite to the measured values, while the predicted values of our model are highly consistent with the experimental. Our model was learned from the five features of

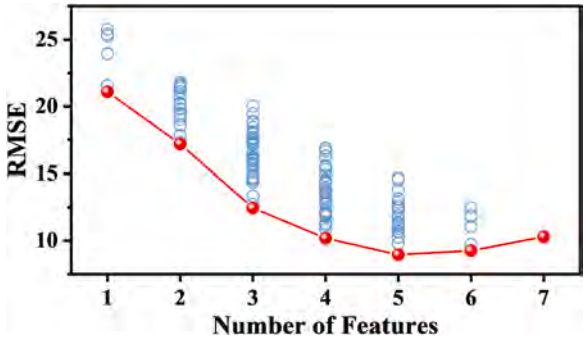

Fig. 5. The predicted error of each subset of features. The red points represent the best models with given feature numbers.

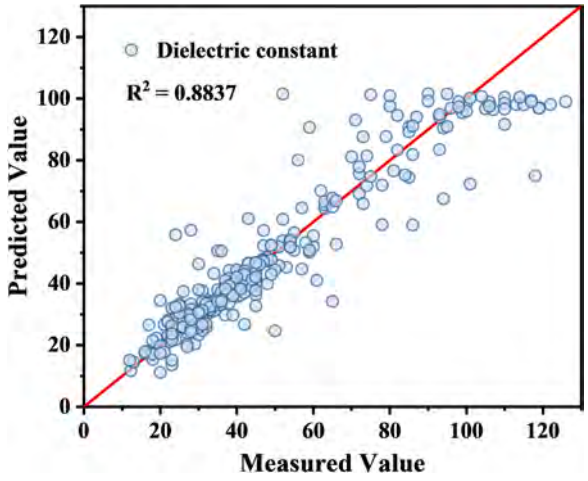

Fig. 6. The dielectric constant prediction via SVR.r algorithm with optimized five features.

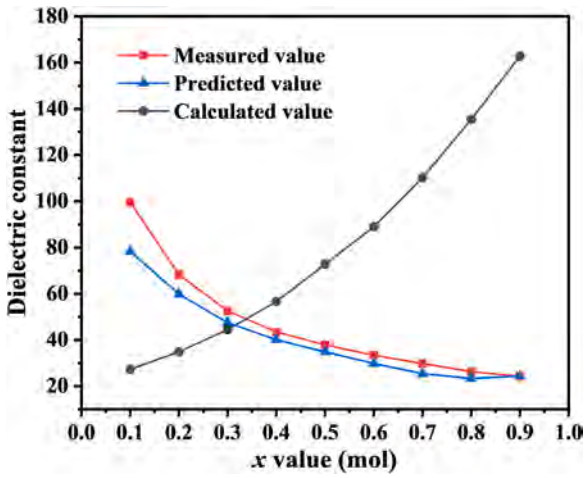

Fig. 7. The measured, predicted, and calculated dielectric constant of $(1-x)CaTiO_3$–$xLa(Mg_{2/3}Nb_{1/3})O_3$ ($x = 0.1$–0.9) ceramics.

arb, eab, epa, emb and ieb while the classical C-M equation mainly considered polarization. There may be some new knowledge. For example, from the perspective of our model, electronegativity is likely to be the key characteristic affecting the dielectric constant, which has also been mentioned in previous literature [44,45]. It is a little pity that we cannot give the exact relationship between electronegativity and dielectric constant due to the limitation of existing dataset. Obviously, the existing results show that in some material systems, our model provides more accurate prediction results than the C-M equation, and we are confident that it will be more widely used in the future.

4. Conclusion and prospects

In summary, we realized the dielectric constant prediction of perovskite microwave dielectric ceramics via machine learning method. The composition and dielectric constant data of 325 perovskite microwave dielectric ceramics were collected, and 25 potential features were constructed based on the composition information. Based on features and target performance, 9 machine learning models were constructed. The best model was used to predict the dielectric constant of materials whose experimental data were inconsistent with the calculated data of C-M equation reported recently. The results verify the reliability of predicting dielectric constant of perovskite microwave dielectric ceramics by our model. We expect that this method can give more accurate dielectric constant prediction results under the condition of greater data volume and higher data quality brought by the combination of experimental data and computational data in the future, and it is hopeful to find the dielectric constant prediction equation of perovskite microwave dielectric ceramics different from the classical equation. Besides, the rapid prediction of dielectric constant, quality factor and resonant frequency temperature coefficient at the same time will greatly accelerate the development efficiency of microwave dielectric ceramics. The prediction of quality factor and temperature coefficient will be will be presented in the next publication.

CRediT authorship contribution statement

Yicong Ye: Conceptualization, Writing – review & editing, Funding acquisition. **Ziqi Ni**: Data curation, Formal analysis, Visualization, Writing – original draft, Writing – review & editing. **Kaijia Hu:** Investigation, Visualization. **Yahao Li**: Methodology. **Yongqian Peng:** Validation. **Xingyu Chen:** Funding acquisition, Supervision, Writing – review & editing.

Declaration of Competing Interest

The authors declare that they have no known competing financial interests or personal relationships that could have appeared to influence the work reported in this paper.

Data Availability

Data will be made available on request.

Acknowledgments

This work is supported by the Natural Science Foundation of Hunan Province of China (Grant No. 2022JJ30661) and the National Natural Science Foundation of China (Grant No. 11705281).

Appendix A. Supporting information

Supplementary data associated with this article can be found in the online version at doi:10.1016/j.mtcomm.2023.105733.

References

[1] M.T. Sebastian, R. Ubic, H. Jantunen, Low-loss dielectric ceramic materials and their properties, Int. Mater. Rev. 60 (2015) 392–412, https://doi.org/10.1179/1743280415Y.0000000007.
[2] H. Yang, S. Zhang, H. Yang, Q. Wen, Q. Yang, L. Gui, Q. Zhao, E. Li, The latest process and challenges of microwave dielectric ceramics based on pseudo phase diagrams, J. Adv. Ceram. 10 (2021) 885–932, https://doi.org/10.1007/s40145-021-0528-4.
[3] J. Fu, High and temperature-stable dielectric constants in PNb_9O_{25} ceramic, J. Am. Ceram. Soc. 105 (2022), https://doi.org/10.1111/jace.18414.
[4] F. Li, Y. Li, J. Zhang, X. Liu, Y. Lu, R. Peng, Y. Liao, T. Tang, X. Wu, Q. Wen, 5G array antenna substrate for electromagnetic beam splitting via cobalt-substituted zinc molybdate low temperature co-fired ceramics, J. Eur. Ceram. Soc. 42 (2022) 5771–5777, https://doi.org/10.1016/j.jeurceramsoc.2022.06.082.
[5] J.Y. Kim, J.-W. Lee, H.S. Jung, H. Shin, N.-G. Park, High-efficiency perovskite solar cells, Chem. Rev. 120 (2020) 7867–7918, https://doi.org/10.1021/acs.chemrev.0c00107.
[6] X. Xu, Y. Pan, L. Ge, Y. Chen, X. Mao, D. Guan, M. Li, Y. Zhong, Z. Hu, V. K. Peterson, M. Saunders, C.-T. Chen, H. Zhang, R. Ran, A. Du, H. Wang, S.P. Jiang, W. Zhou, Z. Shao, High-Performance perovskite composite electrocatalysts enabled by controllable interface engineering, Small Weinh. Bergstr. Ger. 17 (2021), https://doi.org/10.1002/smll.202101573.
[7] M. Shellaiah, K.W. Sun, Review on sensing applications of perovskite nanomaterials, Chemosensors 8 (2020) 55, https://doi.org/10.3390/chemosensors8030055.
[8] D. Yao, M.T. Hoang, H. Wang, Low-Dimensional-Networked perovskites with A-Site-Cation engineering for optoelectronic devices, Small Methods 5 (2021), 2001147, https://doi.org/10.1002/smtd.202001147.
[9] T. Luo, X. Shan, J. Zhao, H. Feng, Q. Zhang, H. Yu, J. Liu, Improvement of quality factor of $SrTiO_3$ dielectric ceramics with high dielectric constant using Sm_2O_3, J. Am. Ceram. Soc. 102 (2019) 3849–3853, https://doi.org/10.1111/jace.16415.
[10] R.V. Leite, F.O.S. Costa, M.T. Sebastian, A.J.M. Sales, A.S.B. Sombra, Experimental and numerical investigation of dielectric resonator antenna based on doped Ba$(Zn_{1/3}Ta_{2/3})O_3$ ceramic, J. Electromagn. Waves Appl. 33 (2019) 84–95, https://doi.org/10.1080/09205071.2018.1526131.
[11] L. Li, X. Ding, Q. Liao, Structure and properties analysis for low-loss $(Mg_{1-x}Co_x)TiO_3$ microwave dielectric materials prepared by reaction-sintering method, Ceram. Int. 38 (2012) 1937–1941, https://doi.org/10.1016/j.ceramint.2011.10.024.
[12] Z. Song, Q. Xu, S. Zhang, H. Liu, W. Luo, H. Hao, M. Cao, Z. Yao, W. Hu, Y. Shi, M. T. Lanagan, The role of microstructure on microwave dielectric properties of (Ba, Sr)TiO_3 ceramics, J. Am. Ceram. Soc. 99 (2016) 905–910, https://doi.org/10.1111/jace.14028.
[13] P.P. Ma, X.Q. Liu, F.Q. Zhang, J.J. Xing, X.M. Chen, $Sr(Ga_{0.5}Nb_{0.5})_{1-x}Ti_xO_3$ low-loss microwave dielectric ceramics with medium dielectric constant, J. Am. Ceram. Soc. 98 (2015) 2534–2540, https://doi.org/10.1111/jace.13655.
[14] Z. Wang, C. Zhai, J. Lu, S. Yin, X. Wang, L. Yu, Structural ordering and microwave dielectric properties of $Ba_{1-x}Ln_{2x/3}(Co_{0.7}Mg_{0.3})_{1/3}Nb_{2/3}O_3$ (Ln═La, Nd) ceramics, Ceram. Int. 44 (2018) 6775–6779, https://doi.org/10.1016/j.ceramint.2018.01.096.
[15] R.D. Shannon, Dielectric polarizabilities of ions in oxides and fluorides, J. Appl. Phys. 73 (1993) 348–366, https://doi.org/10.1063/1.353856.
[16] D.R. Penn, Wave-Number-Dependent dielectric function of semiconductors, Phys. Rev. 128 (1962) 2093–2097, https://doi.org/10.1103/PhysRev.128.2093.
[17] N.M. Ravindra, S. Auluck, V.K. Srivastava, On the penn gap in semiconductors, Phys. Status Solidi B. 93 (1979) K155–K160, https://doi.org/10.1002/pssb.2220930257.

[18] J.H. Gladstone, T.P. Dale, Researches on the refraction, dispersion, and sensitiveness of liquids, Proc. R. Soc. Lond. 12 (1863) 448–453, https://doi.org/10.1098/rspl.1862.0097.
[19] R.A.P. Ribeiro, S.R. de Lazaro, DFT/B3LYP study on structural, electronic and dielectric properties of $SnZr_{0.50}Ti_{0.50}O_3$ lead-free ferroelectric material, J. Alloy. Compd. 714 (2017) 553–559, https://doi.org/10.1016/j.jallcom.2017.04.255.
[20] R. Yuan, Z. Liu, P.V. Balachandran, D. Xue, Y. Zhou, X. Ding, J. Sun, D. Xue, T. Lookman, Accelerated discovery of large electrostrains in $BaTiO_3$-based piezoelectrics using active learning, Adv. Mater. 30 (2018), 1702884, https://doi.org/10.1002/adma.201702884.
[21] J. He, C. Yu, Y. Hou, X. Su, J. Li, C. Liu, D. Xue, J. Cao, Y. Su, L. Qiao, T. Lookman, Y. Bai, Accelerated discovery of high-performance piezocatalyst in $BaTiO_3$-based ceramics via machine learning, Nano Energy 97 (2022), 107218, https://doi.org/10.1016/j.nanoen.2022.107218.
[22] J. Qin, Z. Liu, M. Ma, Y. Li, Machine learning approaches for permittivity prediction and rational design of microwave dielectric ceramics, J. Mater. 7 (2021) 1284–1293, https://doi.org/10.1016/j.jmat.2021.02.012.
[23] E. Kim, J. Kim, K. Min, Prediction of dielectric constants of ABO_3-type perovskites using machine learning and first-principles calculations, Phys. Chem. Chem. Phys. 24 (2022) 7050–7059, https://doi.org/10.1039/D1CP04702G.
[24] J. Deng, G. Jia, An interpretable hybrid machine learning prediction of dielectric constant of alkali halide crystals, Chem. Phys. 555 (2022), 111457, https://doi.org/10.1016/j.chemphys.2022.111457.
[25] K. Wu, N. Sukumar, N.A. Lanzillo, C. Wang, R. Rampi Ramprasad, R. Ma, A. F. Baldwin, G. Sotzing, C. Breneman, Prediction of polymer properties using infinite chain descriptors (ICD) and machine learning: Toward optimized dielectric polymeric materials, J. Polym. Sci. Part B Polym. Phys. 54 (2016) 2082–2091, https://doi.org/10.1002/polb.24117.
[26] Y. Yi, L. Wang, Z. Chen, Adaptive global kernel interval SVR-based machine learning for accelerated dielectric constant prediction of polymer-based dielectric energy storage, Renew. Energy 176 (2021) 81–88, https://doi.org/10.1016/j.renene.2021.05.045.
[27] X. Lin, C. Li, H. Hao, G. Zhao, H. Liu, Accelerated search for ABO_3-type the electronic contribution of polycrystalline dielectric constants by machine learning, Comput. Mater. Sci. 193 (2021), 110404, https://doi.org/10.1016/j.commatsci.2021.110404.
[28] K. Morita, D.W. Davies, K.T. Butler, A. Walsh, Modeling the dielectric constants of crystals using machine learning, J. Chem. Phys. 153 (2020), 024503, https://doi.org/10.1063/5.0013136.
[29] M.T. Sebastian, Dielectric Materials For Wireless Communication, Elsevier, Amsterdam; Boston, 2008.
[30] R. Yuan, Z. Liu, Y. Xu, R. Yin, J. He, Y. Bai, Y. Zhou, J. Li, D. Xue, T. Lookman, Optimizing electrocaloric effect in barium titanate-based room temperature ferroelectrics: combining landau theory, machine learning and synthesis, Acta Mater. 235 (2022), 118054, https://doi.org/10.1016/j.actamat.2022.118054.
[31] R. Yuan, D. Xue, Y. Xu, D. Xue, J. Li, Machine learning combined with feature engineering to search for $BaTiO_3$ based ceramics with large piezoelectric constant, J. Alloy. Compd. 908 (2022), 164468, https://doi.org/10.1016/j.jallcom.2022.164468.
[32] W.M. Haynes, D.R. Lide, T.J. Bruno, CRC Handbook of Chemistry and Physics, CRC, USA, 2014.
[33] E.G. COX, Structural Inorganic Chemistry, Nature 157 (1946) 386–387, https://doi.org/10.1038/157386a0.
[34] N.E. Brese, M. O'Keeffe, Bond-Valence parameters for solids, Acta Crystallogr. B. 47 (1991) 192–197, https://doi.org/10.1107/S0108768190011041.
[35] S.S. Batsanov, 2001. Van der Waals radii of elements, 37 (2001) 15.
[36] R.G. Pearson, Absolute electronegativity and hardness: application to inorganic chemistry, Inorg. Chem. 27 (1988) 734–740, https://doi.org/10.1021/ic00277a030.
[37] K.M. Rabe, J.C. Phillips, P. Villars, I.D. Brown, Global multinary structural chemistry of stable quasicrystals, high-Tc ferroelectrics, and high-Tc superconductors, Phys. Rev. B. 45 (1992) 7650–7676, https://doi.org/10.1103/PhysRevB.45.7650.
[38] L. Pauling, The Nature of the Chemical Bond and the Structure of Molecules and Crystals: an Introduction to Modern Structural Chemistry, Cornell University Press, 1960.
[39] C.E. Moore, 1970. National standard reference data system, 1970.
[40] D.R. Lide, W.M. Haynes, CRC Handbook of Chemistry and Physics: A Ready Reference Book of Chemical and Physical Data, CRC, USA, 2004.
[41] R.D. Shannon, Revised effective ionic radii and systematic studies of interatomic distances in halides and chalcogenides, Acta Crystallogr. Sect. A. 32 (1976) 751–767, https://doi.org/10.1107/S0567739476001551.
[42] X. Chen, W. Zhang, B. Zalinska, I. Sterianou, S. Bai, I.M. Reaney, Low sintering temperature microwave dielectric ceramics and composites based on Bi_2O_3–B_2O_3, J. Am. Ceram. Soc. 95 (2012) 3207–3213, https://doi.org/10.1111/j.1551-2916.2012.05295.x.
[43] X. Song, C. Yin, Z. Zou, J. Yang, F. Zeng, J. Wu, Y. Shi, W. Lu, W. Lei, Structural evolution and microwave dielectric properties of $CaTiO_3$–$La(Mg_{2/3}Nb_{1/3})O_3$ ceramics, J. Am. Ceram. Soc. 105 (2022) 7415–7425, https://doi.org/10.1111/jace.18675.
[44] J.M. Kim, H.W. Jo, E.S. Kim, Effect of electronegativity on microwave dielectric properties of $MgTi_{1-x}(A_{1/3}Sb_{2/3})_xO_3$ ($A = Mg^{2+}$, Zn^{2+}) ceramics, Int. J. Appl. Ceram. Technol. 16 (2019) 2053–2059, https://doi.org/10.1111/ijac.13177.
[45] X.M. Chen, Y. Li, A- and B site cosubstituted $Ba_{6-3x}Sm_{8+2x}Ti_{18}O_{54}$ microwave dielectric ceramics, J. Am. Ceram. Soc. 85 (2002) 579–584, https://doi.org/10.1111/j.1151-2916.2002.tb00135.x.